

## [Supplementary material]

### Neolithic rondels in Central Europe and their builders: an analysis of multi-rondel sites

Václav Vondrovský<sup>1,2,\*</sup>, Lenka Kovačiková<sup>3</sup> & Lubor Smejtek<sup>4</sup>

<sup>1</sup> Institute of Archaeology of the Czech Academy of Sciences, Czech Republic

<sup>2</sup> Institute of Archaeology, Faculty of Arts, University of South Bohemia, Czech Republic

<sup>3</sup> Laboratory of Palaeoecology and Archaeobotany, University of South Bohemia, Czech Republic

<sup>4</sup> Central Bohemian Archaeological Heritage Institute, Czech Republic

\* Author for correspondence ✉ vaclav.vondrovsky@gmail.com

### OSM1: multi-rondel sites

#### *Methodology*

Archaeological excavations and surveys do not usually cover the full extent of the settlement areas of which rondels are a part. Identifying a multi-rondel site—multiple rondel enclosures built within a single settlement area—can therefore be problematic, as even rondels built relatively close to one another could conceivably belong to different settlements. The determination of particular sites in the literature can be misleading because it is often influenced by recent administrative borders. For example, the two rondels labelled Puch and Kleedorf are only 200m apart, but the rondels described as Quedlinburg 1 and Quedlinburg 2 are 5km apart. Co-existence within a single settlement could be assumed in the former case, but hardly in the latter as during this period settlements rarely covered more than 30ha (Řídký *et al.* 2019: 135–43). To mitigate this problem, an arbitrary distance of 1km between the centres of neighbouring enclosures was used as the main factor in defining a multi-rondel arrangement. Where the distance is greater than 1km, the co-existence of these rondels within a single settlement area was declared uncertain and was excluded from the analysis. Also excluded were sites which although presented in the literature as multi-rondel contained other, non-rondel enclosures or earthworks. Two further sites listed as multi-rondel could not be included in the spatial analysis as no details of their attributes have been published.

**Table S1. List of multi-rondel sites. Sites not analysed are marked in grey; the reason for exclusion is indicated. Culture abbreviations: SBK = Stroked Pottery Culture; SOB = Oberlauterbach group; LGK = Lengyel Culture; MOG = Moravian-Austrian Painted Ware.**

Site	Culture	Complex	Rondel count	Reason for exclusion	Source
Bylany	SBK	western	3	–	Pavlů <i>et al.</i> (1995); Křivánek (2019)
Dresden-Nickern	SBK		3	–	Stäuble (2012)
Quedlinburg	SBK		2	5km distance	Northe (2012)
Kolín I	SBK		2	–	Šumberová <i>et al.</i> (2010)
Kolín II	SBK		2	Rondel + non-rondel earthwork	Šumberová <i>et al.</i> (2010)
Kyhna	SBK		4	–	Stäuble (2012)
Lochenice	SBK		2	2km distance	Kovárník (2014)
Praha-Krč	SBK		2	–	–
Vochoz	SBK		2	–	Pavlů & Metlička (2013)
Schmiedorf	SOB		2	–	Trnka (1991)
Friebritz	MOG	eastern	2	–	Melichar & Neubauer (2010)
Glaubendorf	MOG		2	–	Melichar & Neubauer (2010)
Hornsburg	MOG		2	–	Melichar & Neubauer (2010)
Perchtoldsdorf	MOG		2	Details of Perchtoldsdorf 1 unknown	Melichar & Neubauer (2010)
Pranhartsberg	MOG		2	–	Melichar & Neubauer (2010)
Puch – Kleedorf	MOG		2	–	Melichar & Neubauer (2010)
Rechnitz	MOG		2	–	Schiel <i>et al.</i> (2017)
Vedrovice	MOG		2	–	Humpolová (2001)
Villánykövesd	LGK		3?	Details of two enclosures unknown	Bertók & Gáti (2014)
Wilhelmsdorf	MOG		2	1.5km distance	Melichar & Neubauer (2010)
Svodín	LGK		2	–	Němejcová-Pavůvková (1995)
Sormás-Török-földek	LGK		2	Rondel + non-rondel earthwork	Barna & Pásztor (2011)
Szemely-Hegyes	LGK		2	–	Bertók & Gáti (2014)
Zengővárkony-Igaz-dűlő	LGK		2	–	Bertók & Gáti (2014)

**Table S2. Attributes of rondel relations at multi-rondel sites analysed in Figure 3.**

Site	Rondels	Complex	Entrance count identical	Entrance type identical	Entrance orientation identical	Distance between ditches (m)	Distance between centres (m)
Bylany	4/1 + 4/2	western	N	N	N	50	177
Bylany	4/2 + 4/3		N	N	N	235	345
Dresden-Nickern	DD-02 + DD-98		?	N	?	208	273
Dresden-Nickern	DD-98 + NIE-09		?	?	?	188	291
Kolín	1 + 2		Y	N	N	50	197
Kyhna	1 + 2		?	Y	?	247	330
Kyhna	2 + 3		?	Y	?	165	293
Kyhna	3 + 4		?	Y	?	79	190
Praha-Krč	1 + 2		Y	N	N	38	91
Vočov	I + II		?	N	?	173	238
Schmiedorf	1 + 2		N	N	Y	66	131
Friebritz	1 + 2	eastern	N	N	N	494	593
Glaubendorf	1 + 2		N	Y	N	590	669
Hornsburg	1 + 2		Y	N	N	623	719
Pranhartsberg	1 + 2		N	N	N	431	524
Puch – Kleedorf	Puch + Kleedorf		?	?	?	145	232
Rechnitz	1 + 2		Y	Y	Y	438	530
Vedrovice	II + III		N	Y	N	84	224
Szemely-Hegyés	I + II		Y	Y	Y	211	512
Svodín	1 + 2		Y	N	Y	35	9
Zengővárkony-Igaz-dűlő	1 + 2		?	?	?	454	640

**Table S3. Attributes of individual rondels. Entrance classification is described according to Řídký *et al.* (2019: fig. 6.24). Entrance orientation is described according to clock position.**

Rondel	Complex	Ditch count	Innermost ditch diameter (m)	Outermost ditch diameter (m)	Entrance count	Entrance type	Entrance orientation
Bylany 4/1	western	2	90	110	4	22	3-6-9-12
Bylany 4/2		3	86	130	3	34	2-6-10
Bylany 4/3		3	77	114	4	22	1-4-7-10
Dresden-Nickern 1		1	52	–	3	13	2-6-10
Dresden-Nickern 2		2	62	88	4?	25	?
Dresden-Nickern 4		4	68	124	1?	41	?
Kolín 1		4	150	213	4	43	1-4-7-11
Kolín 2		1	82	–	4	12	3-6-9-12
Kyhna 1		3	43	73	?	31	?
Kyhna 2		3	86	107	?	21	?
Kyhna 3		4	77	135	4	44	2-4-8-10
Kyhna 4		2	69	90	3?	21	?
Praha-Krč 1		2	52	66	2	21	3-9
Praha-Krč 2		1	45	–	2	13	2-8
Vochoz I		2	35	49	4	21	9-?
Vochoz II		1	70	–	?	13	?
Schmiedorf 1		3	37	74	4	33	3-6-9-12
Schmiedorf 2		1	52	–	2?	11	9-?
Friebritz 1	eastern	1	110	143	3	25	3-6-12
Friebritz 2		1	53	–	4	11	3-9-11
Glaubendorf 1		1	40	–	2	11	3-9
Glaubendorf 2		3	74	117	5	31	3-5-7-9-11
Hornsburg 1		3	58	106	2	32	2-8
Hornsburg 2		2	61	86	2	21	3-9
Pranhartsberg 1		2	52	75	4	25	1-4-7-10
Pranhartsberg 2		2	75	110	2	26	4-10
Puch		2	60	83	2	21	2-8
Kleedorf		1	107	–	?	11	?
Rechnitz 1		3	40	82	4	35	2-5-8-11
Rechnitz 2		2	71	96	4	25	2-5-8-11

Vedrovice II		1	80	–	4	11	3-6-9-12
Vedrovice III		1	201	–	5	11	1-3-3-8-11
Svodín 1		1	68	–	4	11	1-5-8-11
Svodín 2		2	110	142	4	24	1-5-8-11
Szemely-Hegyes I		1	100	450	4	11	3-6-9-12
Szemely-Hegyes II		3	90	170	4	31	3-6-9-12
Zengővárkony-Igaz-dűlő 1		2	100	170	4	21	3-6-9-12
Zengővárkony-Igaz-dűlő 2		1	250	–	?	?	?

OSM2: radiocarbon dates from Praha-Krč.

Table S4. Radiocarbon dates and their context. Dates related to the LBK occupation are in red.

Lab. code	Radiocarbon age (BP)	Rondel	Part of ditch	Ditch level	Material	Bone weight (g)	Taphonomy	AMS $\delta^{13}C$ (‰)	Collagen (%)	Calibrated date range (95.4% probability)	Notes	
CRL-20122	5891±30	rondel 1	Outer ditch northern part	AB	<i>Bos</i> sp. femur, adult	81	Moderate weathering	-21.5	7.8	4838–4704		
CRL-19938	5767±26			AB	<i>Bos taurus</i> metacarpus, adult	21	No taphonomic effects	-17.0	1.7	4701–4543		
CRL-20123	5891±21			C	<i>Bos taurus</i> scapula, adult	40	Moderate etching	-21.8	5.1	4832–4815 (4.8%) 4801–4712 (90.7%)		
Poz-103998	6170±40			D	Undetermined mammal, undetermined bone (diaphysis)	7	No taphonomic effects	-	5.1	5217–4997		
CRL-19939	5830±26			D	<i>Bos taurus</i> metacarpus, adult	14	No taphonomic effects	-22.1	5.3	4786–4607		
CRL-20325	5826±26			D	<i>Bos taurus</i> tibia, adult	74	No taphonomic effects	-20.1	2.3	4786–4603		
CRL-19935	6205±26		Inner ditch north-eastern part		AB	<i>Bos taurus</i> scapula, adult	35	Moderate abrasion	-19.3	5.2	5292–5266 (5.2%) 5220–5199 (9.1%) 5186–5052 (81.1%)	
CRL-19936	5980±27				C	<i>Bos</i> sp. metatarsus, adult	114	Partial weathering	-19.9	3.8	4947–4787	

CRL-20326	5708±36			C	<i>Bos taurus</i> vertebra cervicali, adult	32	Moderate weathering	-35.5	17.3	4675–4635 (8.0%) 4618–4454 (87.4%)	
Poz-103997	5890±40			D	Large mammal, undetermined bone (diaphysis)	70	No taphonomic effects	-	2.3	4889–4870 (1.6%) 4848–4678 (93.3%) 4630–4622 (0.6%)	
CRL-19937	5929±27			D	<i>Bos taurus</i> tibia, subadult to adult	156	No taphonomic effects	-19.5	4.2	4890–4870 (5.0%) 4848–4721 (90.5%)	
CRL-19514	5772±25	rondel 2	Southern	AB	<i>Bos taurus</i> metacarpus, subadult/adult	17	No taphonomic effects	-23.7	2.5	4699–4546	
CRL-19515	6232±28			C	<i>Ovis/Capra</i> humerus, subadult	9	No taphonomic effects	-21.4	2.8	5304–5244 (33.4%) 5227–5203 (13.5%) 5179–5063 (48.6%)	
CRL-19942	6223±27		Eastern entrance	AB	<i>Bos taurus</i> mandible, adult	26	No taphonomic effects	-18.3	1.6	5301–5251 (21.3%) 5225–5202 (12.0%) 5183–5058 (62.2%)	
CRL-19943	6217±26			D	<i>Bos taurus</i> , mandibular second molar (root)	32	Well preserved	-19.9	6.5	5299–5256 (14.4%) 5222–5201 (10.8%) 5184–5056 (70.2%)	
CRL-19511	5870±29		North-western	AB	<i>Bos primigenius</i> metacarpus, adult	110	Two linked fragments with weathered fracture	-26.6	2.9	4833–4814 (2.7%) 4801–4679 (92.3%) 4628–4624 (0.4%)	
CRL-19512	5943±27			C	<i>Bos taurus</i> pelvis, subadult	99	Well preserved	-25.3	2.7	4901–4863 (14.1%) 4854–4724 (81.4%)	

<i>CRL-19940</i>	5949±28	North-western (feature no. 560)	C	<i>Bos</i> sp. humerus, adult	295	No taphonomic effects	-14.7	5.2	4929–4925 (0.7%) 4905–4726 (94.8%)	
<i>CRL-19513</i>	5842±26		D	<i>Bos primigenius</i> metacarpus, adult	101	Well preserved	-25.6	2.6	4791–4652 (87.0%) 4641–4612 (8.5%)	Identical sample to CRL-19941
<i>CRL-19941</i>	5917±27		D	<i>Bos primigenius</i> metacarpus, adult	94	Well preserved	-20.0	5.2	4878–4874 (0.6%) 4846–4716 (94.6%)	Identical sample to CRL-19513
<i>Poz-102896</i>	5940±35		D	<i>Sus scrofa</i> metapodium, adult	11	No taphonomic effects	–	2.4	4931–4924 (1.0%) 4905–4720 (94.4%)	
<i>CRL-19510</i>	5879±28		–	<i>Bos taurus</i> tibia, subadult/adult	121	Well preserved	-19.9	2.8	4833–4814 (4.2%) 4801–4689 (91.2%)	
<i>CRL-19510r</i>	5950±29		–	<i>Bos taurus</i> tibia, subadult/adult	121	Well preserved	-20.6	2.8	4931–4924 (1.2%) 4905–4726 (94.2%)	Repeated measurement of CRL-19510
<i>CRL-20323</i>	5844±27		–	<i>Bos</i> sp. radius, adult	118	Partially permineralised	-20.3	2.1	4791–4653 (87.9%) 4639–4613 (7.6%)	
<i>CRL-20324</i>	5876±26		–	<i>Bos taurus</i> metacarpus, juvenile	12	No taphonomic effects	-19.5	5.3	4831–4816 (2.5%) 4800–4688 (92.9%)	

### General comments

All samples are from the bones of herbivorous mammals (*Bovidae*, *Ovis/Capra*) except for a small number of dates from the Poznan series, where wild boar and undetermined mammals occur. All samples reached a collagen yield above the 1 per cent threshold (Dobberstein *et al.* 2009). The Czech Radiocarbon Laboratory and Poznan Radiocarbon Laboratory measure %C and %N in the collagen extract and automatically reject dates with C/N ratio >3.6 (DeNiro 1985). The  $\delta^{13}\text{C}$  values were measured during the AMS procedure. They are not compatible with IRMS analysis of stable isotopes referring to diet and environmental conditions.

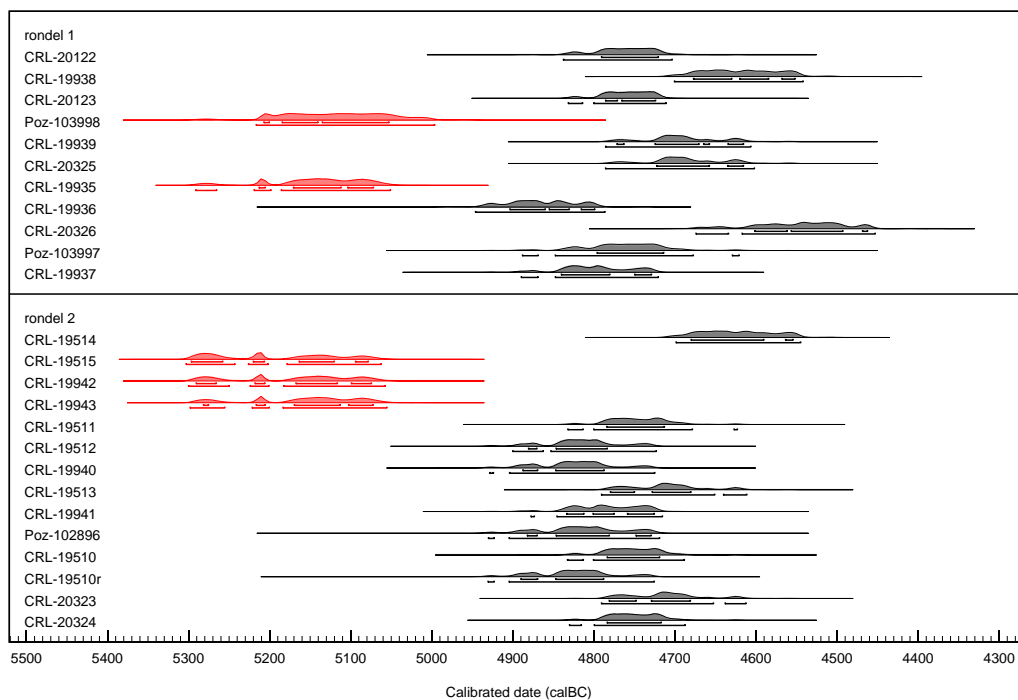
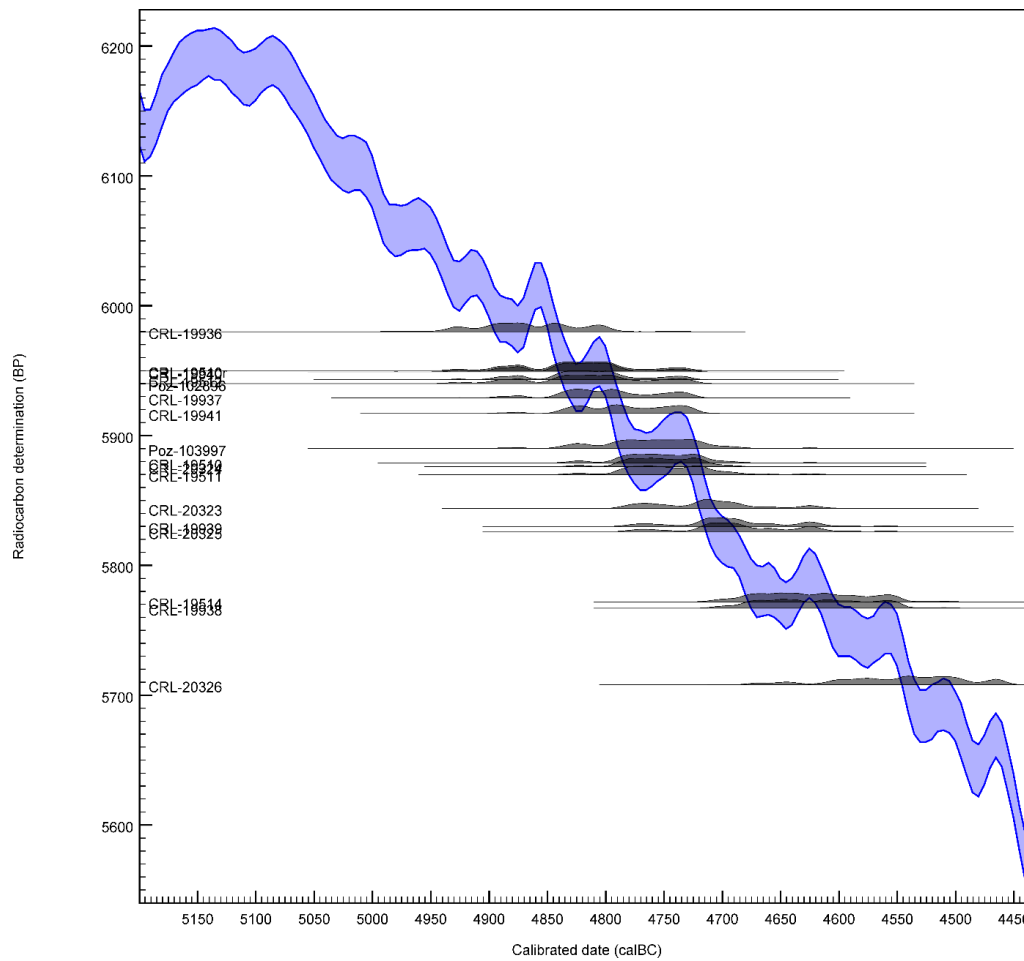


Figure S1. Calibrated dates. Calibrated in OxCal v.4.4. using the IntCal20 calibration curve (Bronk Ramsey 2009; Reimer et al. 2020). Residual dates related to the LBK occupation are in red.



*Figure S2. Curve plot for calibrated radiocarbon dates included in chronological models. Created in OxCal v.4.4. using the IntCal20 calibration curve (Bronk Ramsey 2009; Reimer et al. 2020).*

**OSM3: chronological model for rondel 2.**

**Table S5. Consistency  $\chi^2$ -tests for groups of dates from rondel 2. Groups inconsistent at the 5% significance level are in red.**

Group description	Dates	$\chi^2$ test results
Repeated measurement of sample from pit 560	CRL-19510; CRL-19510r	T = 3.1; T(5%) = 3.8; df = 1
Repeated sampling of bone eroded from pit 560 infill	CRL-19513; CRL-19941	T = 4.0; T(5%) = 3.8; df = 1
Ditch residuals and CRL-19513 eroded from the pit infill	CRL-19512; CRL-19940; Poz-102896; CRL-19513	T = 10.9; T(5%) = 7.8; df = 3
Ditch residuals and CRL-19941 eroded from the pit infill	CRL-19512; CRL-19940; Poz-102896; CRL-19941	T = 0.8; T(5%) = 7.8; df = 3
Dates of pit 560 and CRL-19513 eroded from the pit infill	CRL-19510; CRL-19510r; CRL-20323; CRL-20324; CRL-19513	T = 9.69; T(5%) = 9.5; df = 4
Dates of pit 560 and CRL-19941 eroded from the pit infill	CRL-19510; CRL-19510r; CRL-20323; CRL-20324; CRL-19941	T = 8.6; T(5%) = 9.5; df = 4
Dates from pit 560 and ditch residuals from levels D and C	CRL-19510; CRL-19510r; CRL-20323; CRL-20324; CRL-19941; CRL-19940; CRL-19512; Poz-102096	T = 15.0; T(5%) = 14.1; df = 7
Dates for level AB	CRL-19511; CRL-19514	T = 6.6; T(5%) = 3.8; df = 1
Ditch residuals and CRL-19511 from level AB	CRL-19940; CRL-19512; Poz-102096; CRL-19511	T = 4.9; T(5%) = 7.8; df = 3
Ditch residuals and CRL-19514 from level AB	CRL-19940; CRL-19512; Poz-102096; CRL-19514	T = 32.4; T(5%) = 7.8; df = 3

Although they were extracted from the same bone, CRL-19513 and CRL-19941 are mutually inconsistent. Because CRL-19513 cannot form a homogeneous group either with ditch residuals or with pit 560, this date must be considered unreliable.

### *Model code*

The CQL code for the final model running in OxCal software.

```
Plot("rondel 2")
{
  Sequence()
  {
    Boundary("Start residuals");
    Phase("ditch residuals")
    {
      R_Date("CRL-19512", 5943, 27);
      R_Date("CRL-19940", 5949, 28);
      R_Date("Poz-102896", 5940, 35);
    };
    Boundary("End residuals");
    Boundary("Start pit560");
    Phase("pit560")
    {
      R_Combine("CRL-19510+r")
      {
        R_Date("CRL-19510", 5879, 28);
        R_Date("CRL-19510r", 5950, 29);
      };
      R_Date("CRL-19941", 5917, 27);
      R_Date("CRL-20323", 5844, 27);
      R_Date("CRL-20324", 5876, 26);
    };
    Boundary("End pit560");
    Date("Rondel construction");
    Boundary("Start level AB");
    R_Date("CRL-19514", 5772, 25);
    Boundary("End level AB");
  };
};
```

### Alternative variant A

The sequence simply follows the stratigraphy (feature 560—ditch level D—ditch level C—ditch level AB). Rondel construction is modelled between pit 560 and the ditch sequence.

The CRL-19441 date participates in the pit 560 group.

$A_{\text{overall}} = 34\%$

$A_{\text{model}} = 35\%$

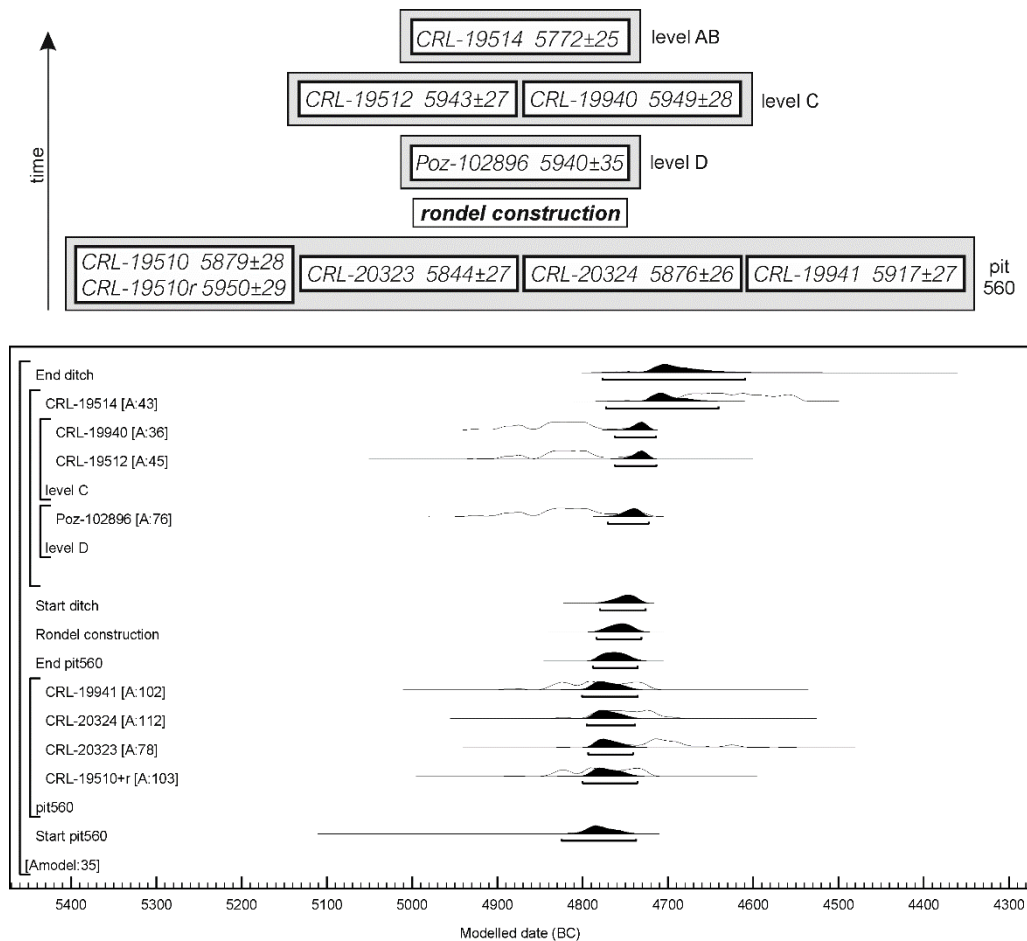


Figure S3. Praha-Krč, rondel 2: alternative model – variant A. Modelled in OxCal v.4.4, using the IntCal20 calibration curve (Bronk Ramsey 2009; Reimer et al. 2020) (figure by V. Vondrovský).

### Alternative variant B

The sequence simply follows the stratigraphy (feature 560—ditch level D—ditch level C—ditch level AB). Rondel construction is modelled between pit 560 and the ditch sequence.

The CRL-19441 date participates in the level D group.

$A_{\text{overall}} = 31\%$

$A_{\text{model}} = 32\%$

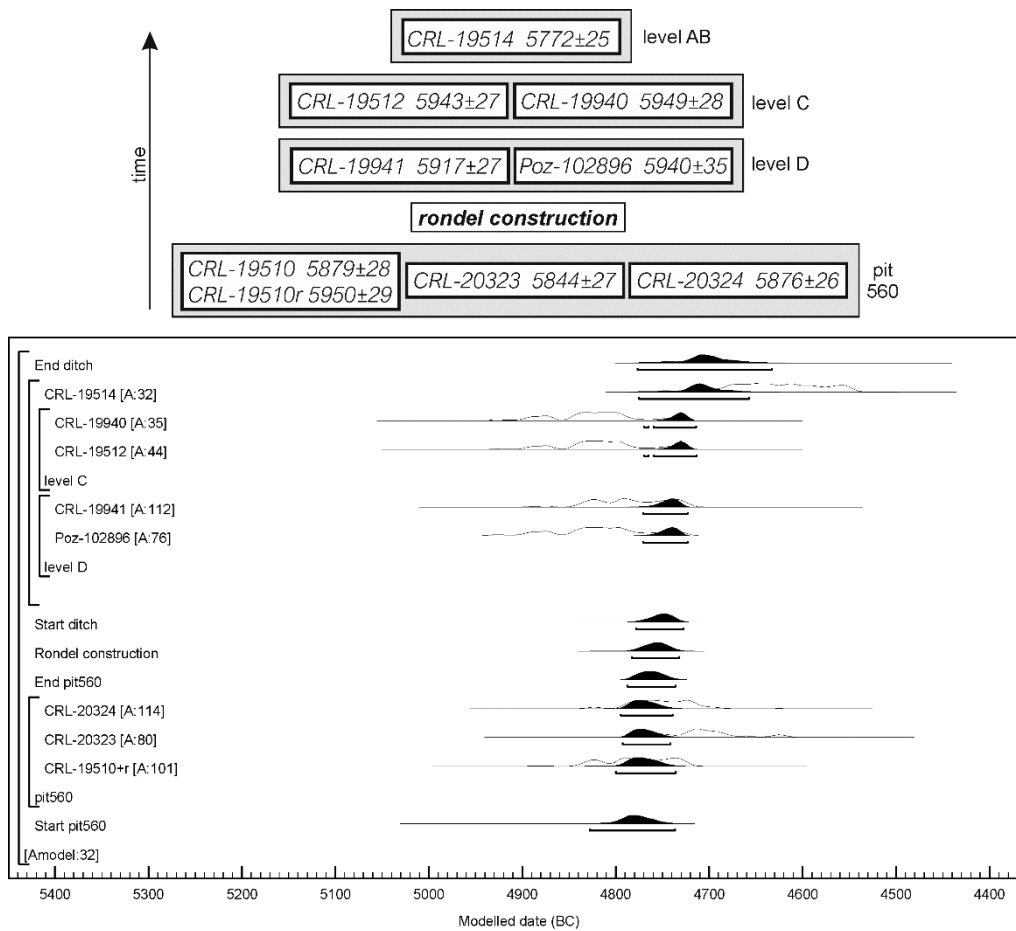


Figure S4. Praha-Krč, rondel 2: alternative model – variant B. Modelled in OxCal v.4.4, using the IntCal20 calibration curve (Bronk Ramsey 2009; Reimer et al. 2020) (figure by V. Vondrovský).

### Alternative variant C

The model examines the possibility that the stratigraphy in the north-western ditch was incorrectly recorded in the field. Therefore, dates from ditch levels C and AB participate in the pit 560 group. The pit is modelled to be younger than the rondel ditch. Only dates from level D belong to the ditch. Rondel construction is positioned at the beginning of the sequence.

$$A_{\text{overall}} = 70\%$$

$$A_{\text{model}} = 76\%$$

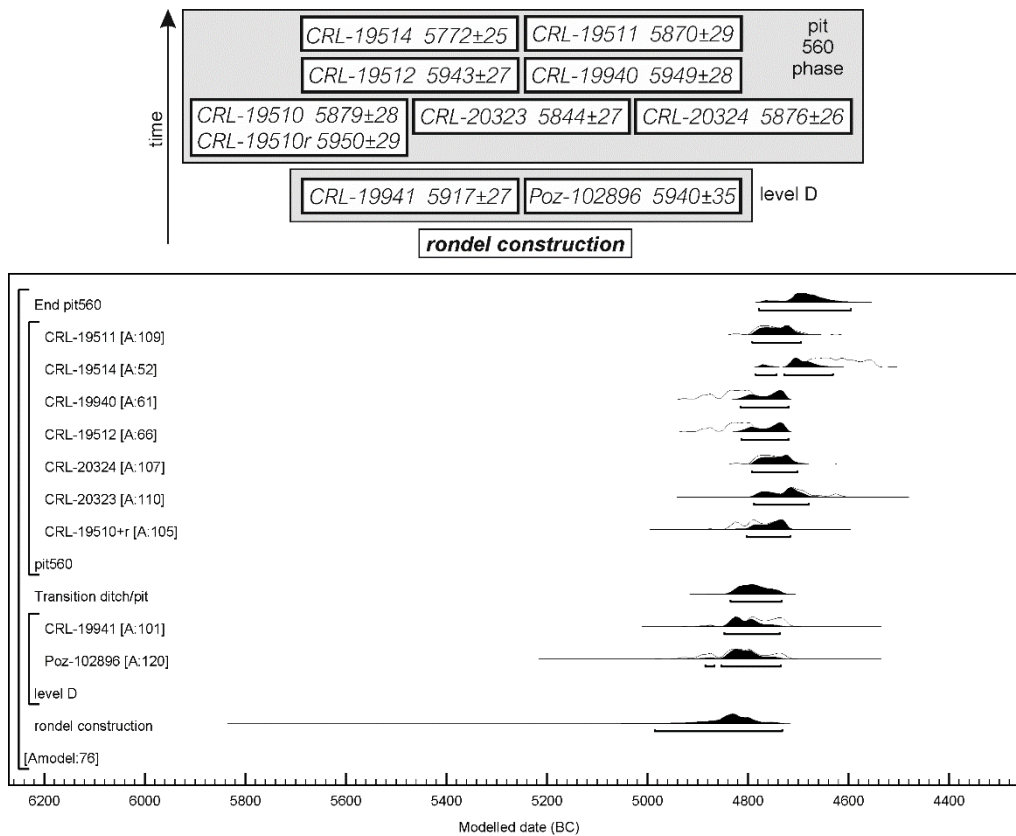


Figure S5. Praha-Krč, rondel 2: alternative model – variant C. Modelled in OxCal v.4.4, using the IntCal20 calibration curve (Bronk Ramsey 2009; Reimer et al. 2020) (figure by V. Vondrovský).

#### Alternative variant D

Pit 560 precedes the rondel ditch. Other samples from ditch levels C and D are assumed to be bones dispersed on the surface not long before rondel construction. This group is therefore younger than storage pit 560. The CRL-19441 date participates in the pit 560 group. The time of rondel construction is modelled between the group of residuals and level AB.

$$A_{\text{overall}} = 49\%$$

$$A_{\text{model}} = 49\%$$

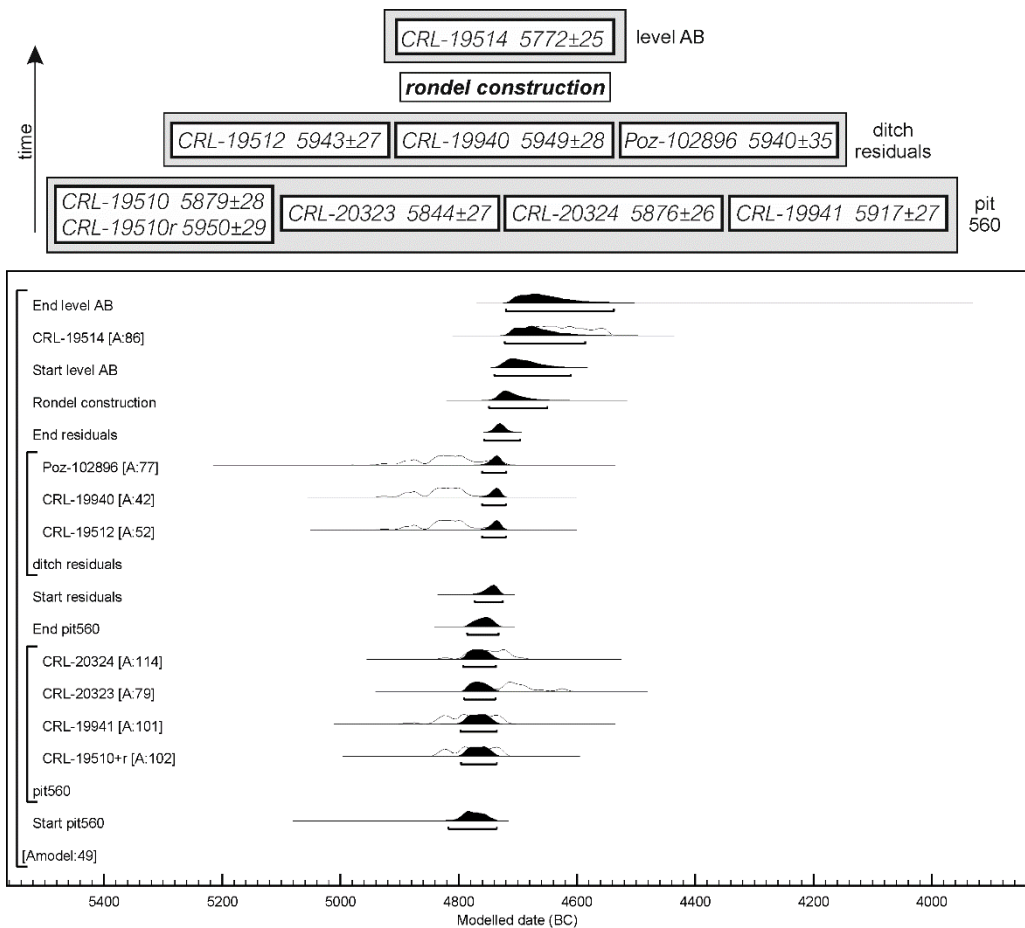


Figure S6. Praha-Krč, rondel 2: alternative model – variant D. Modelled in OxCal v.4.4, using the IntCal20 calibration curve (Bronk Ramsey 2009; Reimer et al. 2020) (figure by V. Vondrovský).

### Alternative variant E

Pit 560 precedes the rondel ditch. Other samples from ditch levels C and D are assumed to be bones dispersed on the surface not long before rondel construction. This group is therefore younger than storage pit 560. The CRL-19441 date participates in the level D group. The time of rondel construction is modelled between the group of residuals and level AB.

$$A_{\text{overall}} = 53\%$$

$$A_{\text{model}} = 53\%$$

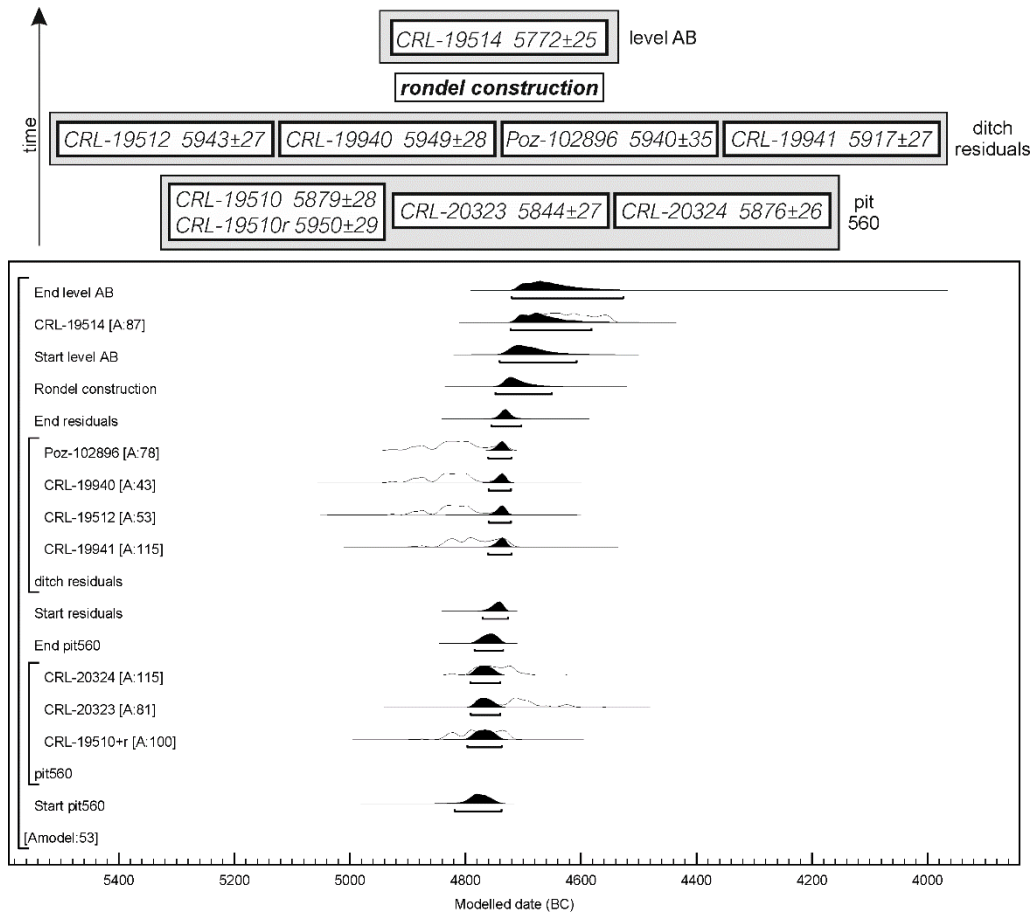


Figure S7. Praha-Krč, rondel 2: alternative model – variant E. Modelled in OxCal v.4.4 using the IntCal20 calibration curve (Bronk Ramsey 2009; Reimer et al. 2020) (figure by V. Vondrovský).

### Alternative variant F

Pit 560 precedes the rondel ditch. Bones in ditch levels D and C are residuals eroded from the rampart. Both dates CRL-19511 and CRL-19514 from ditch level AB mark the infilling of the ditch and the end of rondel use. The time of rondel construction is therefore set between the group of residuals and level AB.

$A_{\text{overall}} = 81\%$

$A_{\text{model}} = 65\%$

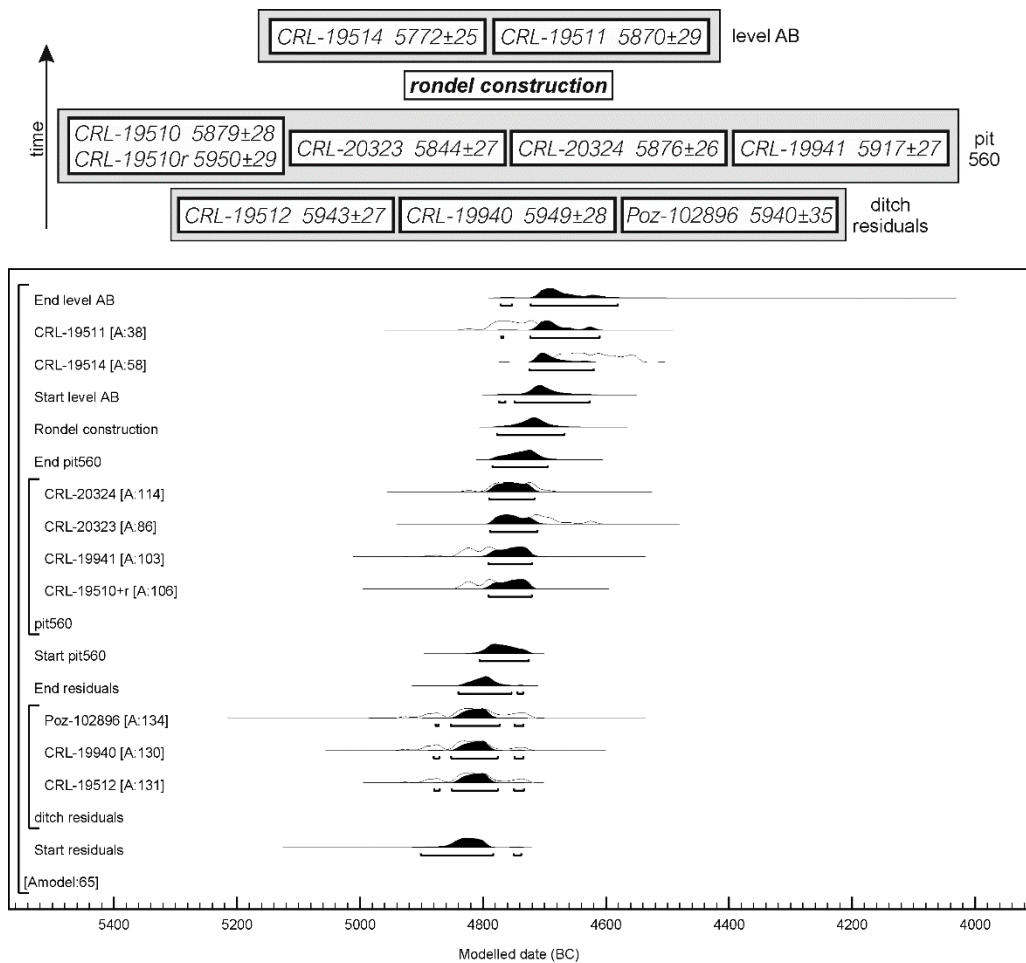


Figure S8. Praha-Krč, rondel 2: alternative model – variant F. Modelled in OxCal v.4.4, using the IntCal20 calibration curve (Bronk Ramsey 2009; Reimer et al. 2020) (figure by V. Vondrovský).

#### Alternative variant G

The alternative model is based on the priors as the final model, but the date CRL-19941 participates in the group of ditch residuals.

$$A_{\text{overall}} = 144\%$$

$$A_{\text{model}} = 145\%$$

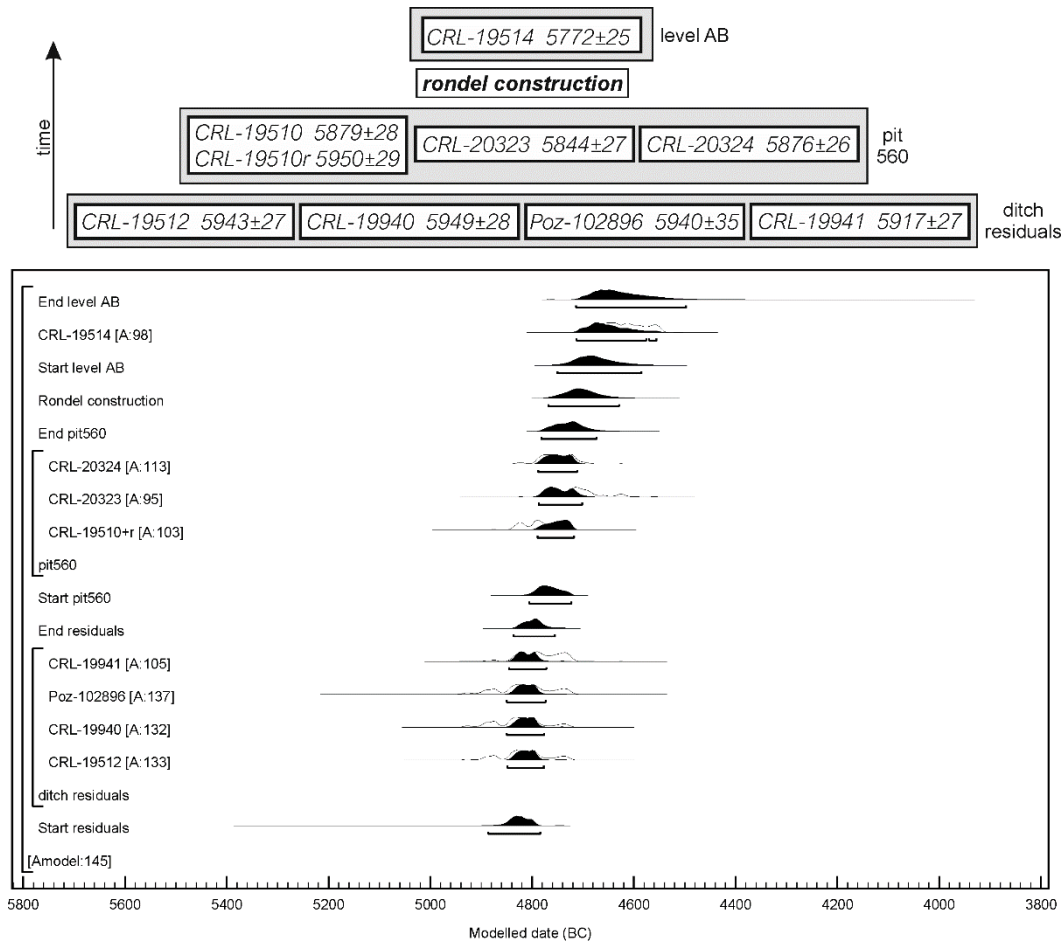


Figure S9. Praha-Krč, rondel 2: alternative model – variant G. Modelled in OxCal v.4.4, using the IntCal20 calibration curve (Bronk Ramsey 2009; Reimer et al. 2020) (figure by V. Vondrovský).

#### OSM4: chronological model for rondel 1.

Table S6. Consistency  $\chi^2$ -tests for groups of dates from the outer ditch of rondel 1.

Groups inconsistent at the 5% significance level are in red.

Group description	Dates	$\chi^2$ -test results
Level AB dates	CRL-19938; CRL-20122	T = 9.8; T(5%) = 3.8; df = 1
Level AB and C dates	CRL-19938; CRL-20122; CRL-20123	T = 15.7; T(5%) = 6.0; df = 2
Potential residuals	CRL-20122; CRL-20123; CRL-19939; CRL-20325	T = 6.3; T(5%) = 7.8; df = 3
Full sequence in the western part of the outer ditch	CRL-19938; CRL-19939; CRL-20325	T = 3.7; T(5%) = 6.0; df = 2
All dates from the outer ditch (except the LBK outlier)	CRL-19938; CRL-19939; CRL-20122; CRL-20123; CRL-20325	T = 17.0; T(5%) = 9.5; df = 4

Dates potentially linked with refuse deposition in the inner and outer ditches	CRL-19938; CRL-20326	$R = 1.8$ ; $T(5\%) = 3.8$ ; $df = 1$
--	----------------------	---------------------------------------

*Model code 1*

The CQL code for the final model of the outer ditch running in OxCal software.

```
Plot("rondel 1 outer")
{
  Sequence()
  {
    Boundary("Start sequence");
    Phase("residuals")
    {
      R_Date("CRL-19939", 5830, 26);
      R_Date("CRL-20325", 5826, 26);
    };
    Boundary("End residuals");
    Date("outer ditch construction");
    Boundary("Start deposition");
    Phase("refuse deposition")
    {
      R_Date("CRL-19938", 5767, 26);
    };
    Boundary("End sequence");
  };
};
```

*Outer ditch: alternative variant A*

The model is based on the “residual-rondel-refuse” sequence incorporating the dates CRL-20122 and CRL-20123 into the residuals group.

$A_{\text{overall}} = 102\%$

$A_{\text{model}} = 105\%$

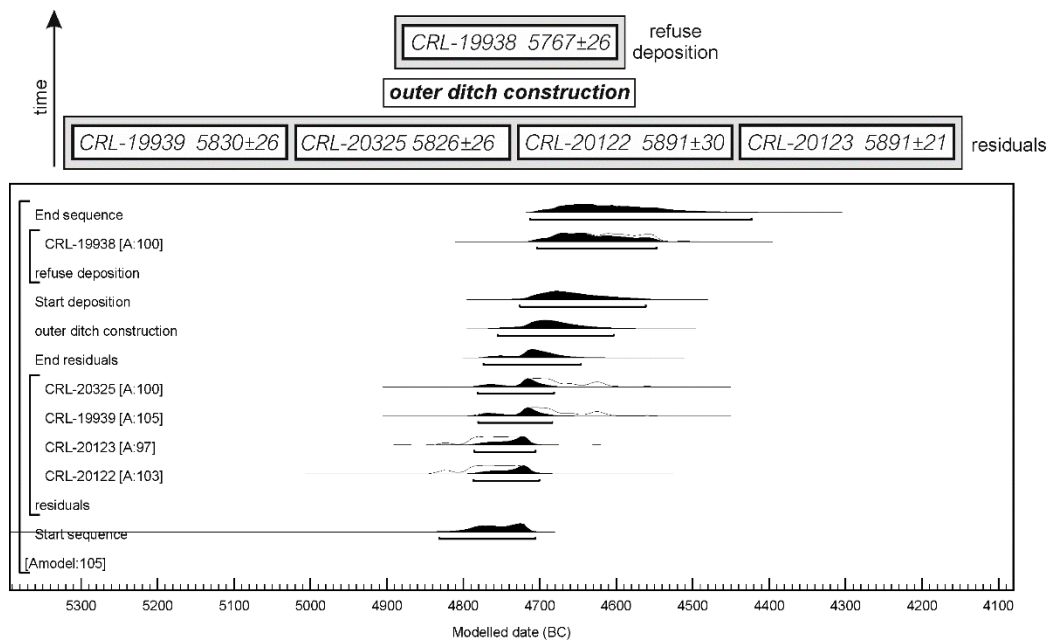


*Figure S10. Praha-Krč, rondel I, outer ditch: alternative model – variant A. Modelled in OxCal v.4.4, using the IntCal20 calibration curve (Bronk Ramsey 2009; Reimer et al. 2020) (figure by V. Vondrovský).*

*Outer ditch: alternative variant B*

A simple sequence following the stratigraphic order of the ditch infill. Levels D and C are considered separate units. Ditch construction is at the beginning of the sequence.

$A_{\text{overall}} = 41\%$

$A_{\text{model}} = 31\%$

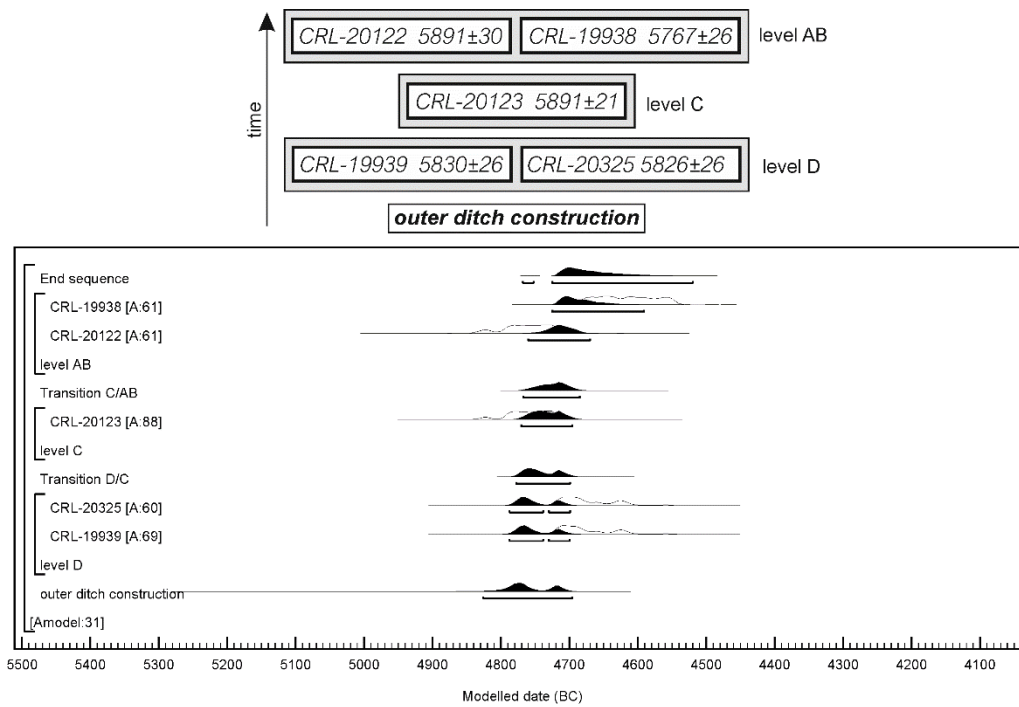


Figure S11. Praha-Krč, rondel 1, outer ditch: alternative model – variant B. Modelled in OxCal v.4.4, using the IntCal20 calibration curve (Bronk Ramsey 2009; Reimer et al. 2020) (figure by V. Vondrovský).

#### Outer ditch: alternative variant C

Level D contains residual material which precedes the ditch building. Infilling of the ditch is represented by all the dates from the find-rich strata of levels C and AB. The time of ditch construction is set between these two groups.

$$A_{\text{overall}} = 37\%$$

$$A_{\text{model}} = 26\%$$

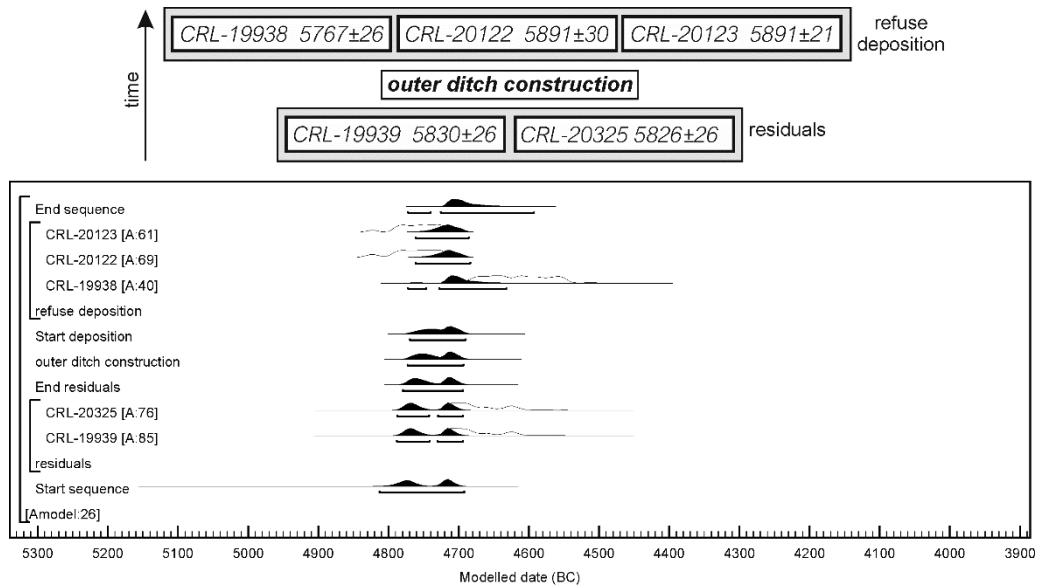


Figure S12. Praha-Krč, rondel 1, outer ditch: alternative model – variant C. Modelled in OxCal v.4.4, using the IntCal20 calibration curve (Bronk Ramsey 2009; Reimer et al. 2020) (figure by V. Vondrovský).

#### Outer ditch: alternative variant D

The layer where sample CRL-20123 was extracted is considered part of level AB in terms of refuse deposition after the rondel decline. Samples from level D are residuals which precede the ditch construction. The time of ditch construction is therefore set between the group of residuals and level AB.

$$A_{\text{overall}} = 34\%$$

$$A_{\text{model}} = 22\%$$

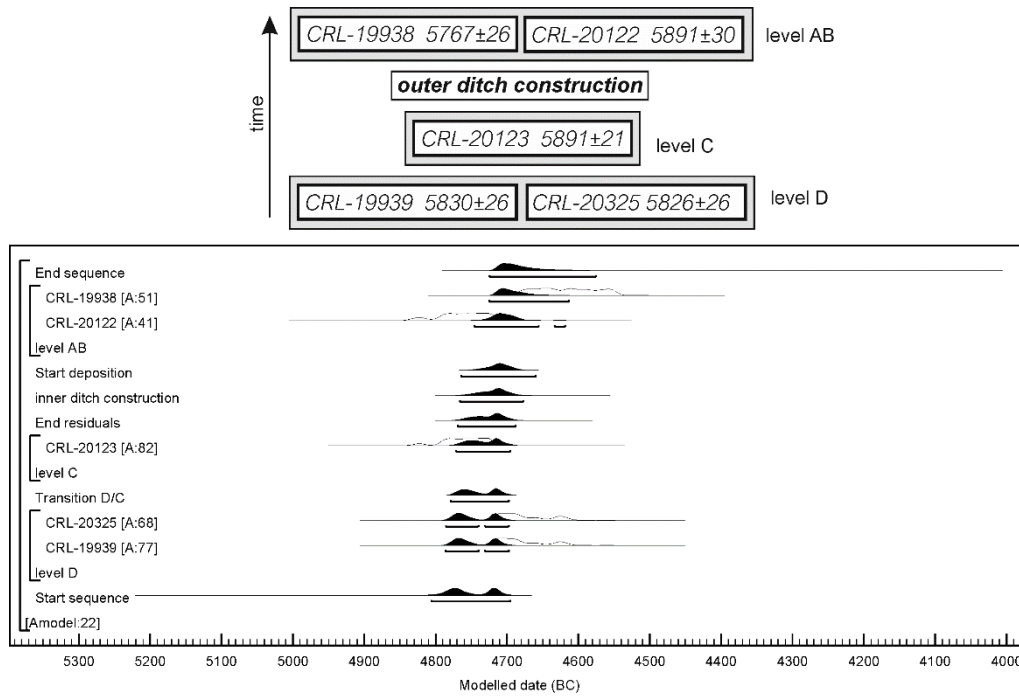


Figure S13. Praha-Krč, rondel 1, outer ditch: alternative model – variant D. Modelled in OxCal v.4.4, using the IntCal20 calibration curve (Bronk Ramsey 2009; Reimer et al. 2020) (figure by V. Vondrovský).

Table S7. Consistency  $\chi^2$ -tests for groups of dates from the inner ditch of rondel 1. Groups inconsistent at the 5% significance level are in red.

Group description	Dates	$\chi^2$ -test result
Level C dates	CRL-19936; CRL-20326	T = 36.2; T(5%) = 3.8; df = 1
Level D dates	CRL-19937; Poz-103997	T = 0.7; T(5%) = 3.8; df = 1
Ditch residuals	CRL-19936; CRL-19937; Poz-103997	T = 3.9; T(5%) = 6.0; df = 2
All dates from the inner ditch (except the LBK outlier)	CRL-19936; CRL-19937; CRL-20326; Poz-103997	T = 37.9; T(5%) = 7.8; df = 3

*Model code 2*

The CQL code for the final model of the inner ditch running in OxCal software.

```
Plot("rondel 1 inner")
{
  Sequence()
  {
    Boundary("Start sequence");
    Phase("residuals")
    {
      R_Date("CRL-19937", 5929, 27);
      R_Date("Poz-133997", 5890, 40);
      R_Date("CRL-19936", 5980, 27);
    };
    Boundary("End residuals");
    Date("inner ditch construction");
    C_Date("outer ditch simulation", -4659, 34);
    Boundary("Start deposition");
    Phase("refuse deposition")
    {
      R_Date("CRL-20326", 5708, 36);
    };
    Boundary("End sequence");
  };
};
```

### *Inner ditch: alternative variant A*

The model is constructed according to the “residual-rondel-refuse” sequence, but the date CRL-20326 is considered a residual. The stratigraphic order of residuals is preserved. Inner ditch construction follows residuals and precedes the outer ditch construction.

$$A_{\text{overall}} = 30\%$$

$$A_{\text{model}} = 26\%$$

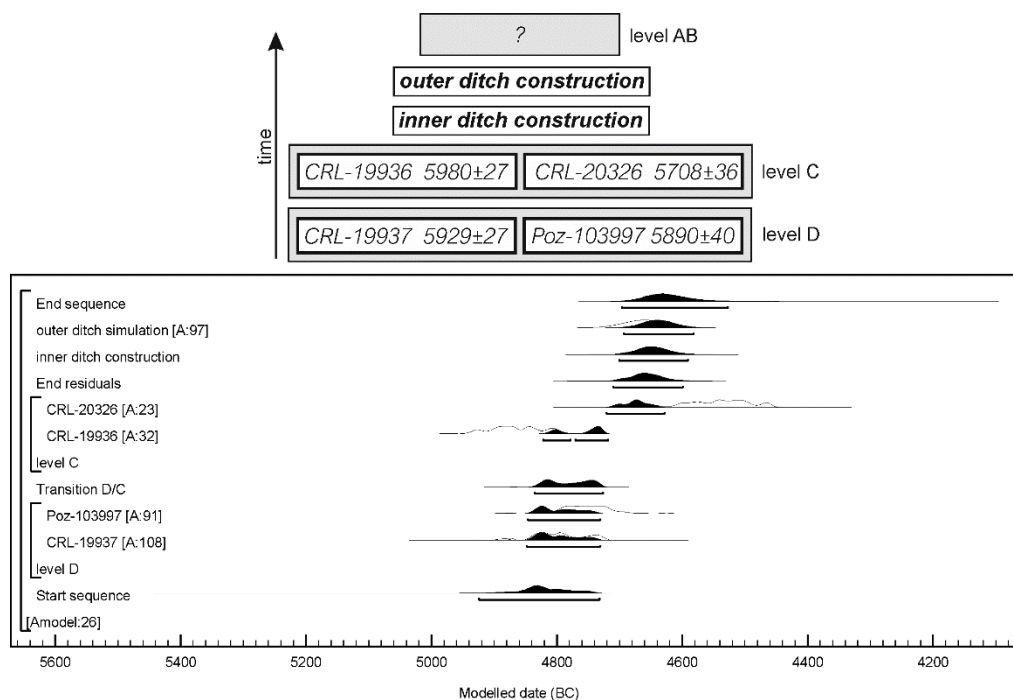


*Figure S14. Praha-Krč, rondel 1, inner ditch: alternative model – variant A. Modelled in OxCal v.4.4, using the IntCal20 calibration curve (Bronk Ramsey 2009; Reimer et al. 2020) (figure by V. Vondrovský).*

### *Inner ditch: alternative variant B*

A simple sequence following the stratigraphic order of the ditch infill, respecting levels D and C as separate units. Ditch construction is situated at the beginning of the sequence, assuming that all dates originate in the period after the ditch was constructed.

$$A_{\text{overall}} = 53\%$$

$$A_{\text{model}} = 48\%$$

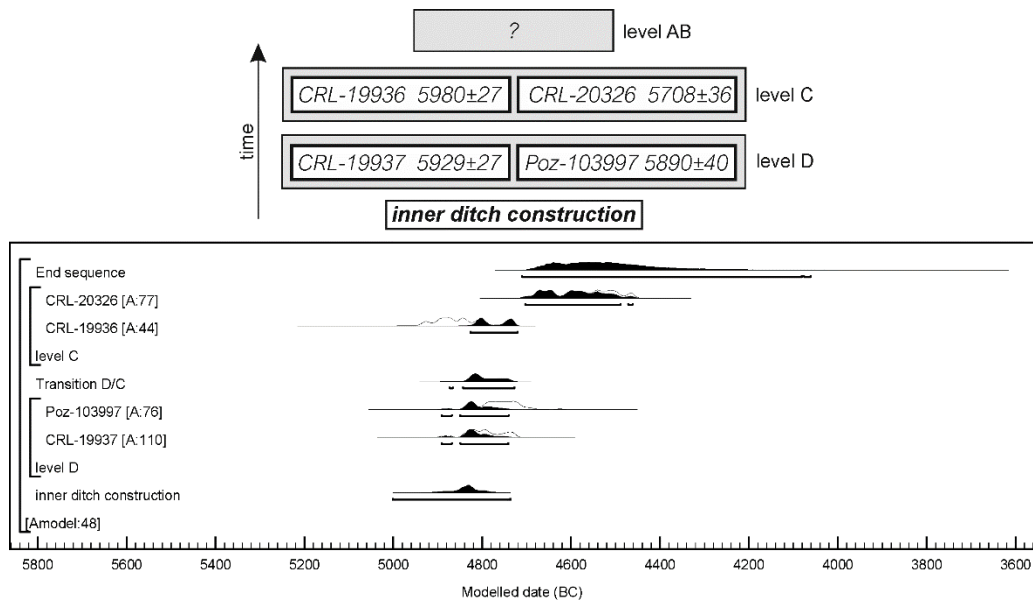


Figure S15. Praha-Krč, rondel 1, inner ditch: alternative model – variant B. Modelled in OxCal v.4.4, using the IntCal20 calibration curve (Bronk Ramsey 2009; Reimer et al. 2020) (figure by V. Vondrovský).

### Inner ditch: alternative variant C

The model is constructed according to the “residual-rondel-refuse” sequence, but the date CRL-20326 is considered a residual. The stratigraphic order of residuals is not respected. Inner ditch construction follows residuals and precedes the construction of the outer ditch.

$A_{\text{overall}} = 49\%$

$A_{\text{model}} = 47\%$

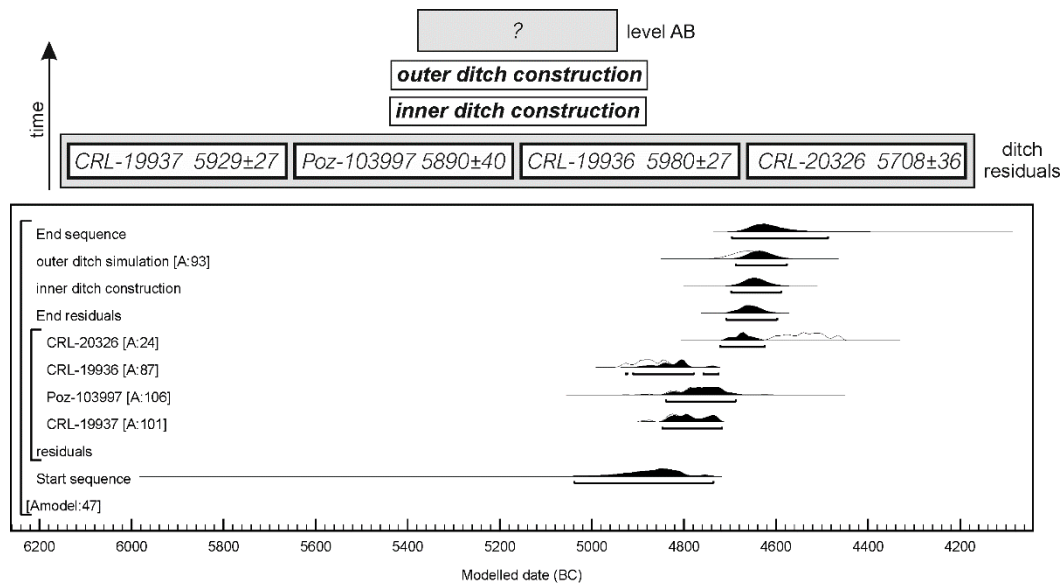


Figure S16. Praha-Krč, rondel 1, inner ditch: alternative model – variant C. Modelled in OxCal v.4.4, using the IntCal20 calibration curve (Bronk Ramsey 2009; Reimer et al. 2020) (figure by V. Vondrovský).

### Inner ditch: alternative variant D

The model is constructed according to the “residual-rondel-refuse” sequence. The date CRL-20326 represents intentional refuse deposition and the date CRL-19936 from the same level is considered a residual. The stratigraphic order of residuals is respected. Inner ditch construction follows residuals and precedes the outer ditch construction.

$A_{\text{overall}} = 66\%$

$A_{\text{model}} = 62\%$

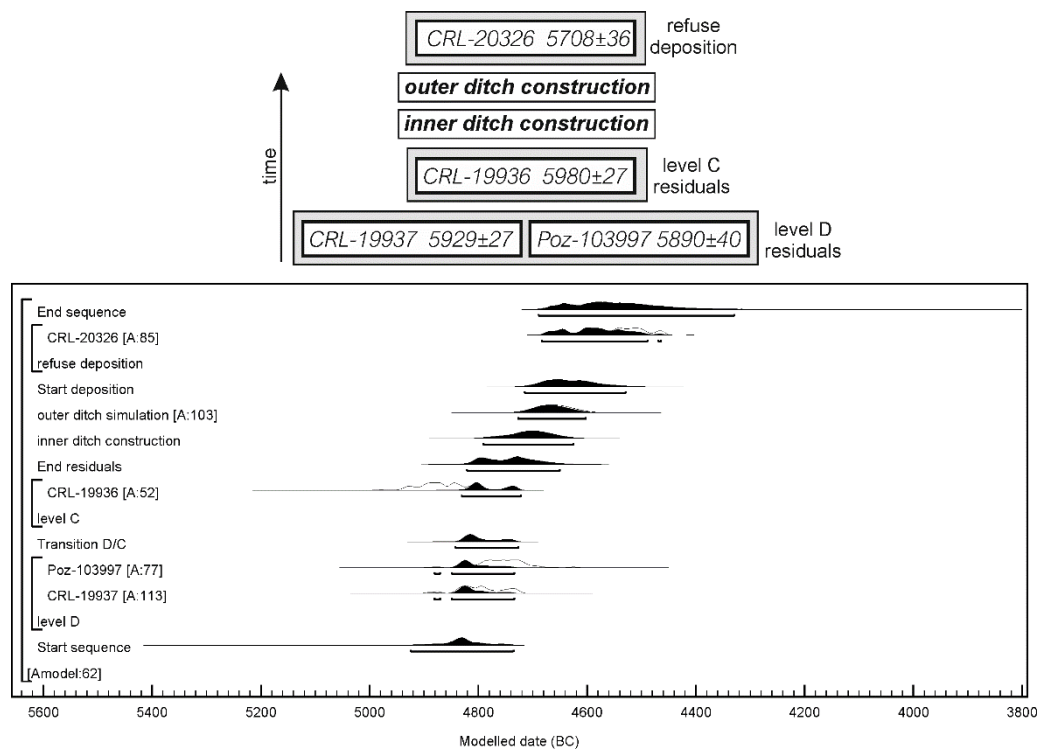


Figure S17. Praha-Krč, rondel 1, inner ditch: alternative model – variant D. Modelled in OxCal v.4.4, using the IntCal20 calibration curve (Bronk Ramsey 2009; Reimer et al. 2020) (figure by V. Vondrovský).

## References

- BARNA, J.P. & E. PÁSZTOR. 2011. Different ways of using space: traces of domestic and ritual activities at a Late Neolithic settlement at Sormás-Török-földek. *Documenta Praehistorica* 38: 185–206. <https://doi.org/10.4312/dp.38.15>
- BERTÓK, G. & C. GÁTI. 2014. *Old times–new methods: non-invasive archaeology in Baranya County (Hungary) 2005–2013*. Budapest: Archaeolingua.
- BRONK RAMSEY, C. 2009. Bayesian analysis of radiocarbon dates. *Radiocarbon* 51: 337–60. <https://doi.org/10.1017/S0033822200033865>
- DENIRO, M.J. 1985. Postmortem preservation and alteration of in vivo bone collagen isotope ratios in relation to palaeodietary reconstruction. *Nature* 317: 806–809. <https://doi.org/10.1038/317806a0>
- DOBBERSTEIN, R.C. *et al.* 2009. Archaeological collagen: why worry about collagen diagenesis? *Archaeological and Anthropological Sciences* 1: 31–42. <https://doi.org/10.1007/s12520-009-0002-7>

- HUMPOLOVÁ, A. 2011. Rondeloid číslo III lidu s Moravskou malovanou keramikou ve Vedrovicích, in V. Podborský (ed.) *30 let archeologických výzkumů Masarykovy university na Znojemsku*: 157–66. Brno: Masarykova univerzita.
- KOVÁRNÍK, J. 2014. Nové objevy kruhových příkopů ve východních Čechách: Poznámka k mladoneolitickým rondelům. *Archeologie západních Čech* 8: 16–33.
- KŘIVÁNEK, R. 2019. The contribution of new geophysical measurements at the previously excavated Neolithic rondel area near Bylany, central Bohemia. *Archaeological Prospection* 27: 39–52. <https://doi.org/10.1002/arp.1755>
- MELICHAR, P. & W. NEUBAUER. 2010. *Mittelneolithische Kreisgrabenanlagen in Niederösterreich: geophysikalisch-archäologische Prospektion: ein interdisziplinäres Forschungsprojekt*. Wien: Österreichischen Akademie der Wissenschaften.
- NĚMEJCOVÁ-PAVÚKOVÁ, V. 1995. *Svodín: zwei Kreisgrabenanlagen der Lengyel-Kultur*. Bratislava: Filozofická fakulta Univerzity Komenského.
- NORTHE, A. 2012. Quedlinburg: zwei Kreisgrabenanlagen in Nordharzvorland, in F. Bertemes & H. Meller (ed.) *Neolithische Kreisgrabenanlagen in Europa. Internationale Arbeitstagung 7.–9. Mai 2004 in Goseck*: 89–104. Halle: Landesamt für Denkmalpflege und Archäologie Sachsen-Anhalt.
- PAVLŮ, I. & M. METLIČKA. 2013. *Neolitický sídelní areál ve Vochově*. Praha: Archeologický ústav AV ČR.
- PAVLŮ, I., J. RULF & M. ZÁPOTOCKÁ. 1995. Bylany rondel: model of the Neolithic site. *Památky archeologické* 3: 7–123.
- REIMER P.J. *et al.* 2020. The IntCal20 Northern Hemisphere radiocarbon calibration curve (0–55 kcal BP). *Radiocarbon* 62: 725–57. <https://doi.org/10.1017/RDC.2020.41>
- ŘÍDKÝ, J. *et al.* 2019. *Big men or chiefs? Rondel builders of Neolithic Europe*. Oxford: Oxbow. <https://doi.org/10.2307/j.ctv13nb7k7>
- SCHIEL, H. *et al.* 2017. Large-scale high-resolution magnetic prospection of the KGA's Rechnitz, Austria, in B. Jennings, C. Gaffney, T. Sparrow & S. Gaffney (ed.) *12<sup>th</sup> International Conference of Archaeological Prospection*: 215–17. Oxford: Archaeopress.
- STÄUBLE, H. 2012. Stichbandkeramische Kreisgrabenanlagen aus Sachsen: neues zu einem alten Thema?, in F. Bertemes & H. Meller (ed.) *Neolithische Kreisgrabenanlagen in Europa. Internationale Arbeitstagung 7.–9. Mai 2004 in Goseck*: 135–58. Halle: Landesamt für Denkmalpflege und Archäologie Sachsen-Anhalt.

ŠUMBEROVÁ, R., D. MALYKOVÁ, J. VEPŘEKOVÁ & M. PECINOVÁ. 2010. Sídlní aglomerace v prostoru dnešního Kolína. Záchranný výzkum v trase obchvatu města. *Archeologické rozhledy* 87: 61–103.

TRNKA, G. 1991. *Studien zu mittelneolithischen Kreisgrabenanlagen* (Mitteilungen der Prähistorischen Kommission der Österreichischen Akademie der Wissenschaften 26). Wien: Österreichischen Akademie der Wissenschaften.